Project:

Integrated Aeroservoelastic Uncertainty/Damage Tolerance/Reliability of Composite Aircraft

Subtopic:

Wind Tunnel Model Development for Aeroelastic Tests of Wing / Control-Surface Systems with Hinge Stiffness Loss and with a Velocity-Squared Damper

Francesca Paltera* and Mark Tuttle**
And
Eli Livne***

The Center of Excellence for Advanced Materials in Transport Aircraft Structures (AMTAS)
University of Washington, Seattle, WA

A Progress Report presented at the FAA Joint Advanced Materials and Structures Center of Excellence (JAMS) Meeting, May 2010, Seattle, WA.

Introduction

Adverse aeroelastic and aeroservoelastic behavior due to variability, damage, or failure of structural components is a concern that must be addressed in the design of modern aircraft. Causes and consequences of such aeroelastic and aeroservoelastic behavior must be well understood, and reliable numerical modeling supported by experimental results must be available to aircraft designers, certifiers, and operators. With support from the FAA and the Boeing Company, work at the University of Washington in recent years was aimed at expanding knowledge and development of simulation tools and experimental capabilities that would contribute to the aeroelastic / aeroservoelastic design of composite aircraft. A number of R&D directions were pursued simultaneously: (a) The aeroelasticity of uncertain composite airframes subject to variability in material properties, material degradation in service and damage, as well as inspection and repair practices, (Refs. 2,6,10,11);(b) Efficient simulation of nonlinear structural aeroelastic behavior of optimized pristine and damaged composite airframes due to large deformations, including buckling of local and global components, (Refs, 1,3,4,5,7,8,9); (c) Simulation and design of composite airframes with control surface free-play and other hinge nonlinearities (Ref. 12), and (d) the development of aeroelastic wind tunnel testing capabilities at the University of Washington that would lead to tests using large aeroelastic models in the UW's Kirsten 12' x 8' wind tunnel (Refs. 6,12) in support of FAA and industry needs.

A significant body of work has been reported over the last 50 years on the problem of aeroelastic response of aerospace systems with stiffness free-play. Simulation work at Duke University supported by a significant number of aeroelastic wind tunnel tests in the Duke's 2' x 2' low speed wind tunnel covered flutter, limit cycle oscillations (LCO), and gust response of a simple wing / control-surface system, including studies of the application of active control in the linear and nonlinear aeroelastic cases. These studies (Refs. 13-20) exposed the complexity of even a

---

* Graduate student, Department of Mechanical Engineering
** Professor and chair, Department of Mechanical Engineering
***Professor, Department of Aeronautics and Astronautics

relatively simple aeroelastic system when structural nonlinearities appear and provided valuable simulation and experimental data that are very useful to developers of commercial level nonlinear aeroelastic simulation tools. Work at Boeing (Refs. 21,22) pursued the development of commercial simulation tools for aircraft with control systems free-play that are suitable for handling problems involving large numbers of degrees of freedom.

Of particular interest to the airplane designer is the case of loss of control surface structural hinge stiffness. Such loss of hinge stiffness may be caused by actuator failure or structural failure of the actuator support structure or the control surface structure to which the actuator is attached. To prevent catastrophic aeroelastic failure in such a case nonlinear hinge rotation dampers are used. Such dampers should, desirably, provide low damping at low rates of rotation of the control surface on its hinge, thus interfering only minimally with the flight control system. As rotation speeds of the control surface become larger due to loss of stiffness, the nonlinear actuators provide increasing level of damping so as to dissipate larger and larger amounts of energy and limit the oscillation amplitude. The result can be limit cycle oscillation (LCO). Commonly used nonlinear dampers are of the velocity-squared type. That is, they provide damping forces which are proportional to the square of the velocity of relative motion.

There is, however, no aeroelastic test data that would allow validation of simulation results for the control surface no-stiffness / velocity-squared damping case. It has been the goal of the FAA/Boeing supported AMTAS work in recent months to develop an aeroelastic wind tunnel model and carry out tests that would allow measurement of the aeroelastic behavior of such a system. Much effort has been spent this year on the design and testing of a small nonlinear damper. The present paper is a work in progress report on the status of this effort.

The University of Washington's Tail/Rudder (Wing/Control-Surface) Aeroelastic Model

An aeroelastic tail/rudder model for wind tunnel tests in the University of Washington's 3 x 3 low speed wind tunnel was built to replicate a design developed by the aeroelasticity research group at Duke University (Refs. 13-14). The terms wing/control-surface and tail/rudder can be used interchangeably here. The model is made of an aluminum tail (wing) attached to the wind tunnel vertically by a support structure that allows plunging and pitching motions. A rudder (control-surface) is attached to the wing along a hinge line. It is made of composite materials. Leaf springs provide plunge stiffness. Rotational springs provide rotational stiffness for the tail about the tail's elastic axis and for the rudder on its hinge. The model allows installation of different rudders made of different skin layups and core construction, including damaged rudders. Ballast masses allow variation of the tail's (wing) inertial properties. The model is shown in Figures 1-5.

One of a series of rudder designs produced is shown in Figure 6. The manufacturing process for that particular rudder utilized 3 plies of Epoxy/Carbon Fibers Pre-preg with a stack sequence of [90°,0°,90°] with the 0° fibers parallel to the span length. Two half section of the composite skin were laid-up and cured over an aluminum mandrel. The mandrel was machined using a CNC mill and it ensured the desired shape to the rudder.

The model was used to assess the effects of various types of rudder damage on the flutter speed of the system. It was also used for aeroelastic tests involving rudder hinge stiffness free-play to validate and confirm predictions by aeroelastic simulation codes developed. Both flutter instability and limit cycle oscillations (LCO) at different flow conditions were measured in the wind tunnel and correlated with numerical predictions.

Note (Figure 5) that the model includes installation points for different actuators or dampers that would simulate rudder actuators and dampers on a real flight vehicle.

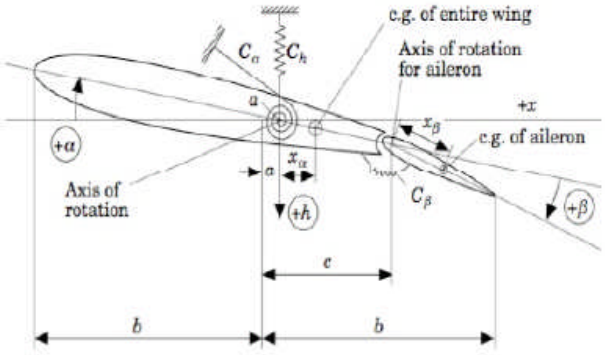

Figure 1 Schematic of the aeroelastic model

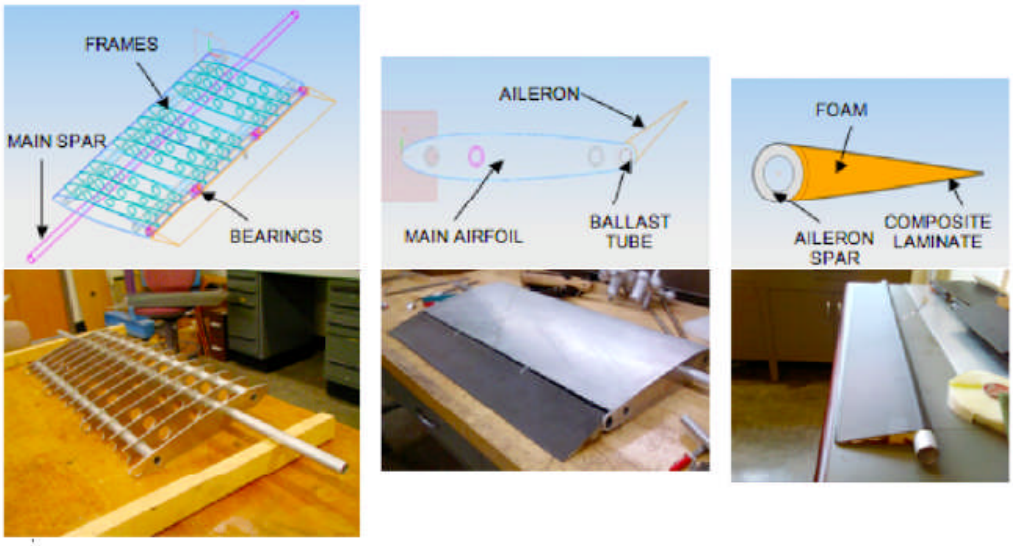

Figure 2 Design and manufacturing of the model

Figure 3 Support Blocks

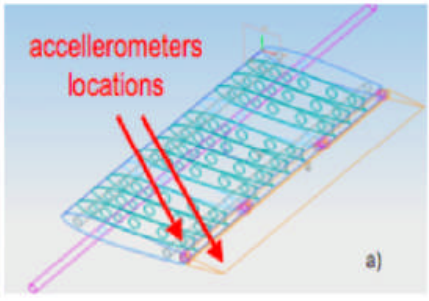

Figure 4 Accellerometers Location

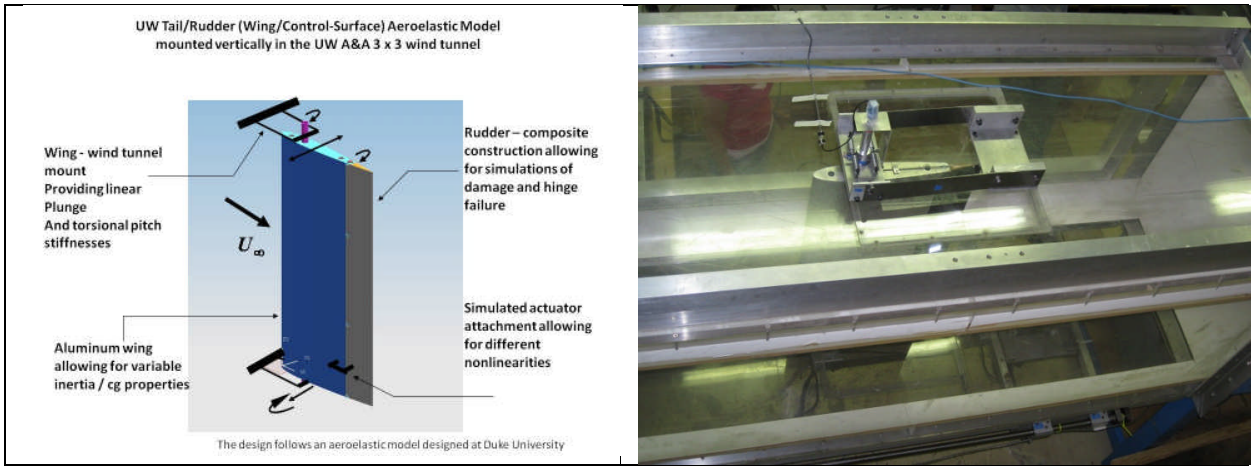

Figure 5: The Aeroelastic Tail/Rudder Model

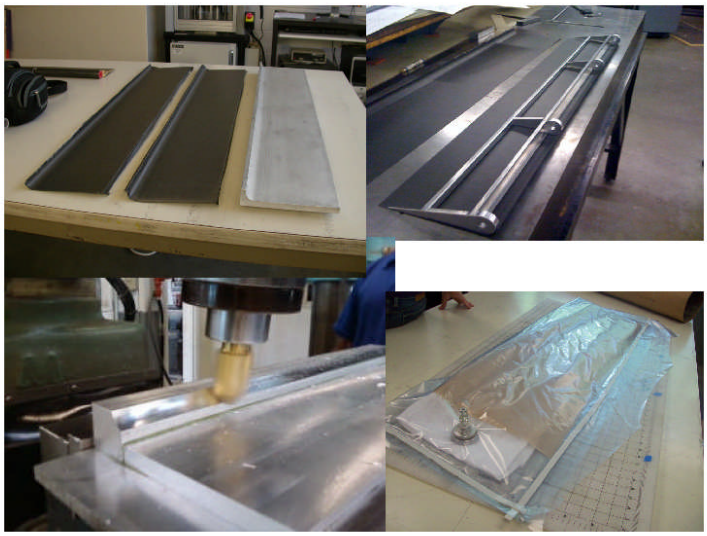

Figure 6: A sample rudder design

The Actuator Failure / Velocity-Squared Damper Case

An important condition in the aeroelastic design and certification of lifting-surface / control-surface systems is the case of loss of actuator stiffness, with control surface rotation resisted only by a velocity-square damper. Studies of this case at Boeing using the aeroelastic wing/control-surface system of Ref. 13 are presented in Ref. 22, from which Figures 7-9 are taken to demonstrate the complexity of the resulting behavior.

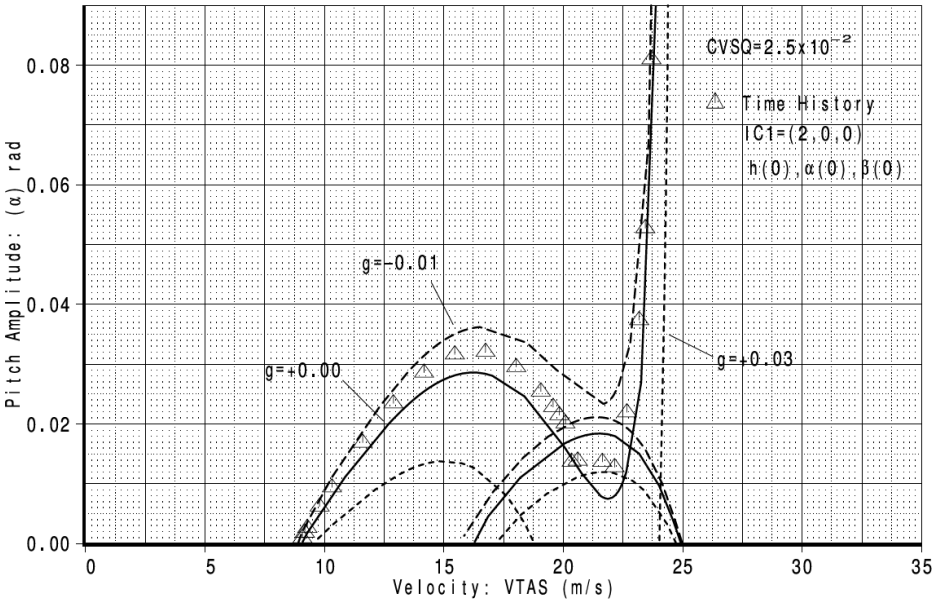

Figure 7: Limit Cycle Oscillation tail pitch amplitude vs. air speed with zero hinge stiffness and a velocity-squared hinge damper (Dr. James Gordon, Boeing, Ref. 22).

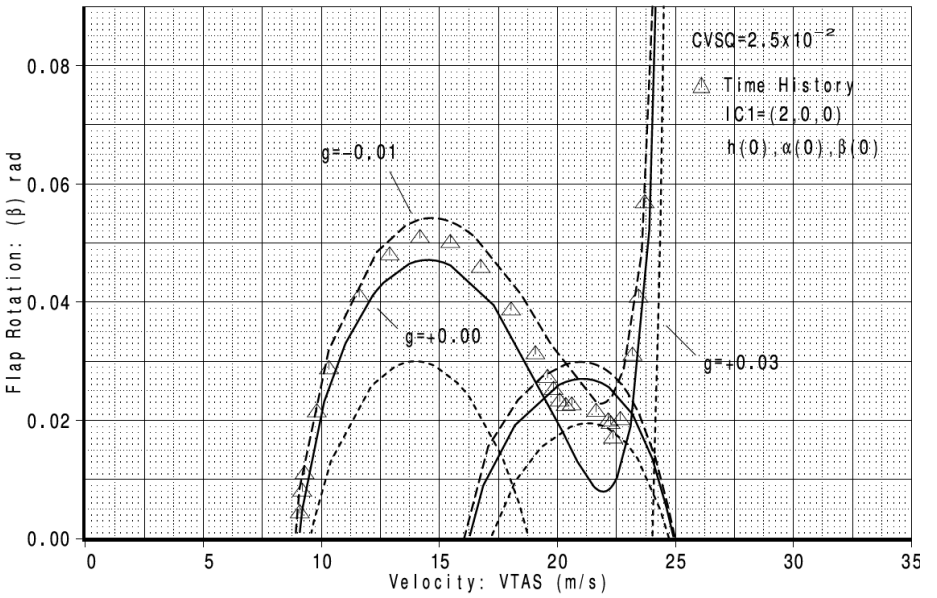

Figure 8: Limit Cycle Oscillation (LCO) rudder rotation amplitude vs. air speed with zero hinge stiffness and a velocity-squared hinge damper (Dr. James Gordon, Boeing, Ref. 22).

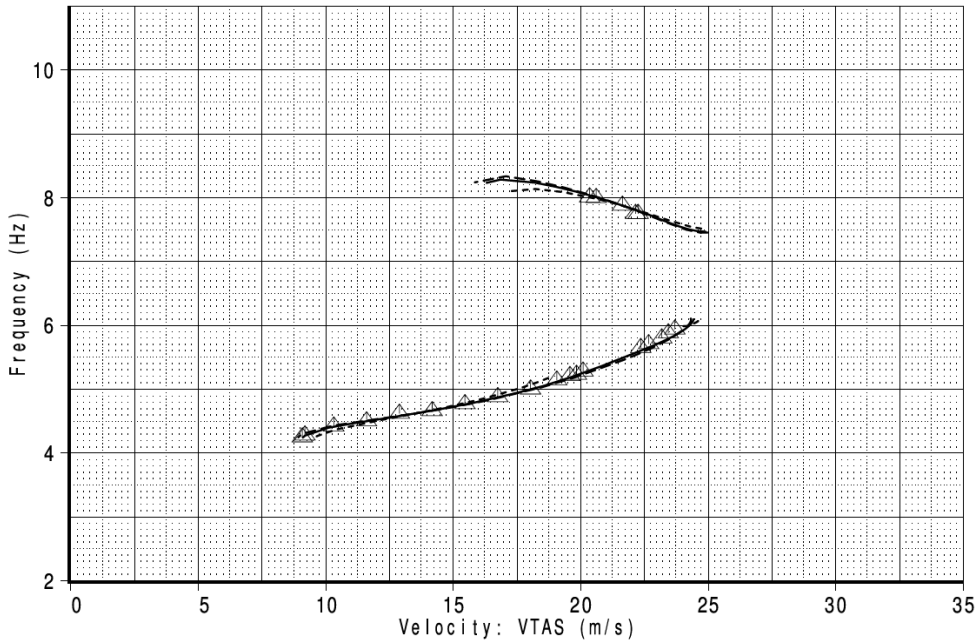

Figure 9: Limit Cycle Oscillation (LCO) frequency vs. air speed with zero hinge stiffness and a velocity-squared hinge damper (Dr. James Gordon, Boeing, Ref. 22).

Figures 7-9 show possible LCO solutions obtained by a Describing Function method (lines), as well as solutions obtained using time domain simulations (triangles). Not all possible LCO solutions obtained by the DF method are stable. That is, the system may not be able to sustain stable LCO oscillations at all points on the lines in Figs. 7-9. The time domain solution, if based on many time domain simulations with extensive coverage of the possible initial conditions involved, usually reflect actual behavior as measured in the wind tunnel.

Figures 7-9 show that in the particular case analyzed the system is stable up to a speed of about 9 m/sec. In response to disturbance below this speed the system will return to zero in the absence of other excitations. Above 9 m/sec the system responds to initial condition disturbances with limit cycle oscillations of increasing magnitude. The LCO magnitude reaches a maximum at about 16 m/sec, then gets lower, reaches a minimum around a speed of about 22 m/sec, and then increases again until complete flutter is reached at about 24 m/sec.

At a speed of about 21 m/sec the frequency of the LCO motions switches from about 5.1 Hz to 8 Hz. It then switches back to 5.5 Hz around a speed of 22 m/sec.

Additional results for the simple Duke University system are presented in Ref. 22. Similar simulations must be carried out for real configurations involving control surface stiffness free-play and actuator failure in the design and certification of all aircraft.

The Development of a Small Velocity-Squared Actuator for Aeroelastic Tests at the University of Washington's 3 x 3 Low Speed Wind Tunnel

After an unsuccessful search for off the shelf dampers that would exhibit velocity-squared force behavior, and another unsuccessful attempt to obtain information regarding design details of existing full scale dampers from

their manufacturers, a prototype damper was designed and built at the University of Washington, and tests were carried out to study its characteristics. The damper was designed to be based on the Bernoulli equation, where a piston with specially designed orifices is moving in a cylinder full of fluid. Acceleration of the fluid through the orifices in the piston head leads to pressure differences between the two sides of the piston head that are proportional to piston to cylinder relative velocity squared according to the theory. Actual implementation adds uncertainties in the form of hysteresis due to force lagging behind the motion as the piston reverses direction with respect to the cylinder and eddy currents in the fluid are formed. Friction forces between the circumference of the piston head and the inside wall of the cylinder as well as due to friction between the piston rod and the seals through which it moves are also present and have to be modeled.

Simple mathematical models for hydraulic / pneumatic dampers were developed for the case of incompressible fluids and the case of compressible fluids – water or air, respectively, in the range of velocities and forces expected in the case of the current tail/rudder aeroelastic model.

A Mathematical Model of a Hydraulic Velocity-Squared Damper (The Incompressible Fluid Case)

The key assumptions used in developing the simple mathematical model used for the design of the damper are (not in any particular order of importance) that orifices are not too small, the piston's speed is not too high, fluid is incompressible, the Bernoulli effect is dominant (and viscous losses at the orifices are small), the cylinder is long relative to the motion amplitude of the piston, cylinder end effects can be neglected, and that orifices are designed and distributed so that pressure on each side of the piston is uniform. It was expected that corrections would be needed to account for end effects and the non-uniform flow patterns around the piston's head and at the end walls of the cylinder. Numerically modeling those effects was left to subsequent CFD modeling of the flow field inside the cylinder.

Properties and mathematical symbols used for the first prototype built at the University of Washington (Figure 10)**:**

Diameter Cylinder Dc = 0.03567 m
Diameter Piston Dp = 0.03377 m
Diameter Orifice Do = 0.0043656 m
Number of Orifices = 4
Thickness Piston Head t = 0.00952 m
Free Play Between Cylinder and Piston h = (Dc-Dp)/2
Water Density ρ = 1000 kg/m^3
Water Viscosity μ = 0.001 Pa*s
Mass rod+piston $m_{piston/rod}$ = 58 g
Piston Velocity v_p (m/s)
Frequency tested f (Hz)
Amplitude tested A (m)

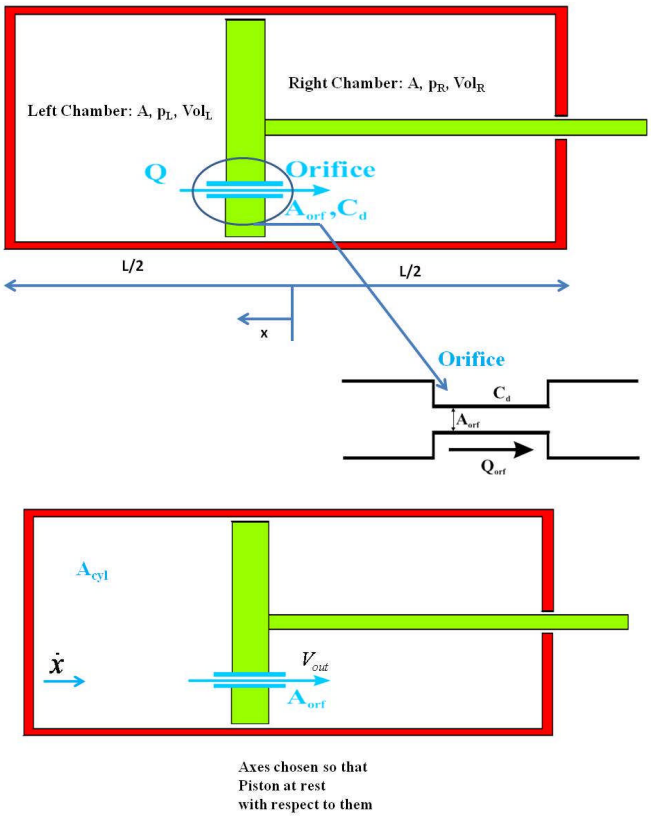

Figure 10: The Principle of Hydraulic Velocity-Squared Damper Design (Figures based on "On the Modeling of Hydraulic Components in Rotorcraft Systems" By Olivier A. Bauchau and Haiying Liu, *School of Aerospace Engineering*, *Georgia Institute of Technology.)*

Application of Bernoulli's equation (piston moving to the left with speed v_p) in a reference frame to the piston: On the far left the flow at the wall (moving toward the piston) has a velocity $\dot{x}$ and pressure p_L. Out of the orifice to into the chamber right of the piston the flow is accelerated to V_{out} and the pressure is p_R. Bernoulli's equation (assuming no viscous-friction loss inside the orifice and an incompressible fluid) leads to

$$p_L + \frac{1}{2}\rho \cdot {v_p}^2 = p_R + \frac{1}{2}\rho \cdot {V_{out}}^2 \rightarrow \Delta p = p_R - p_L = \frac{1}{2}\rho \cdot ({V_{out}}^2 - {v_p}^2)$$

The subscripts L and R denote left chamber and right chamber, respectively.

The cross sectional area of the piston is A_p. The cross sectional area of the orifice is $A_{orifice}$.

Conservation of volume flux (and mass, since the fluid is incompressible) requires that the volume change per unit time due to the motion of the piston into the left chamber will be equal to the volume flowing from left to right through the orifice:

$$A_p \cdot v_p = A_{orifice} \cdot V_{out} \rightarrow V_{out} = \left(\frac{A_p}{A_{orifice}}\right) \cdot v_p = \frac{1}{\eta} \cdot v_p$$

where:

$$\eta = \frac{A_o}{A_p} = 0.0668$$

Then, eliminating V_{out} from the Bernoulli equation

$$\Delta p = \frac{1}{2}\rho \cdot v_p{}^2 \cdot \left(\frac{1}{\eta^2} - 1\right)$$

The force due to pressure difference on the piston is:

$$F_{pressure} = A \cdot \Delta p = (A_{piston} - A_{orifices}) \cdot \Delta p = (1-\eta) \cdot A_{piston} \cdot \frac{1}{2}\rho \cdot v_p{}^2 \cdot \left(\frac{1}{\eta^2} - 1\right)$$

Then:

$$\boxed{F_{pressure} = \frac{(1-\eta)\cdot(1-\eta^2)}{\eta^2} \cdot \frac{1}{2}\rho \cdot A_p \cdot v_p{}^2 = 93.1018 \cdot v_p{}^2}$$

The shear stress on piston head's circumference due to viscous actions between the cylinder wall and the piston is:

$$\tau = \mu \cdot \frac{\partial v}{\partial y} = \mu \cdot \frac{v_p}{h}$$

The force due to viscosity is:

$$F_{viscosity} = A_p \cdot \tau = \pi \cdot D_p \cdot t \cdot \tau$$

Then:

$$\boxed{F_{viscosity} = \pi \cdot D_p \cdot t \cdot \mu \cdot \frac{v_p}{h} = 0.1063e^{-2} \cdot v_p}$$

Also, the force due to the piston and rod inertia is:

$$F_{inertial} = m_{piston/rod} \cdot \varpi^2 \cdot A$$

Then:

$$\boxed{F_{inertial} = (2 \cdot \pi \cdot f)^2 \cdot A \cdot m_{piston/rod}}$$

So, the total force due to damping and inertia is:

$$F_{tot} = F_{pressure} + F_{viscosity} + F_{inertial}$$

A typical force versus velocity curve for the prototype damper is shown in Figure 11 for simple harmonic motion imposed the damper.

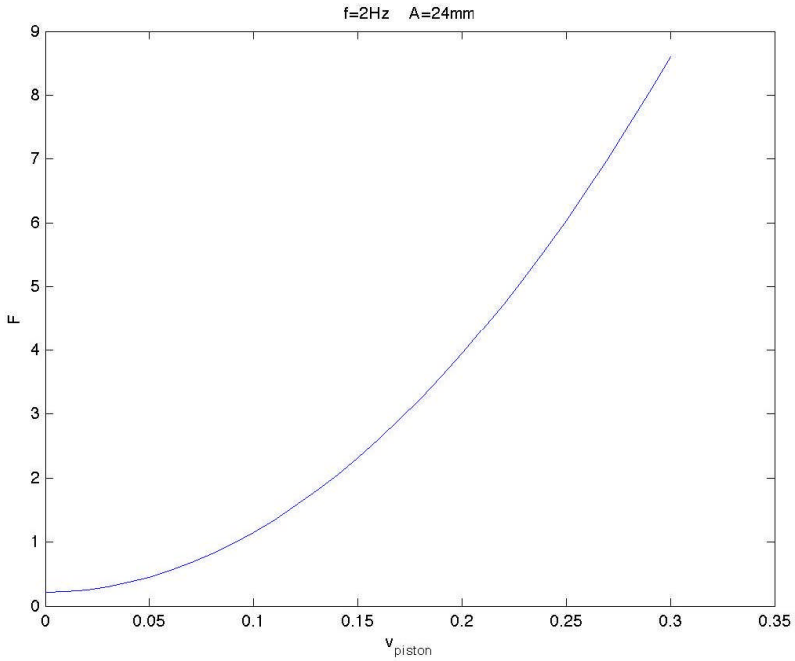

Figure 11: Representative force-velocity relations for the damper in simple harmonic motion

Prototype Damper and Tests

Pictures of the prototype damper are shown in Figure 12. The damper allows for changes in design of its piston head and its orifices shapes and distribution.

Figure 12: The prototype damper

Tests of the damper were carried out in an Instron machine in two configurations: direct attachment of the damper to the machine, which limited the stroke that could be tested (Fig. 13). Alternatively, a system of levers was designed for attaching the damper to the machine in a way that would allow testing of larger amplitudes (Fig. 14).

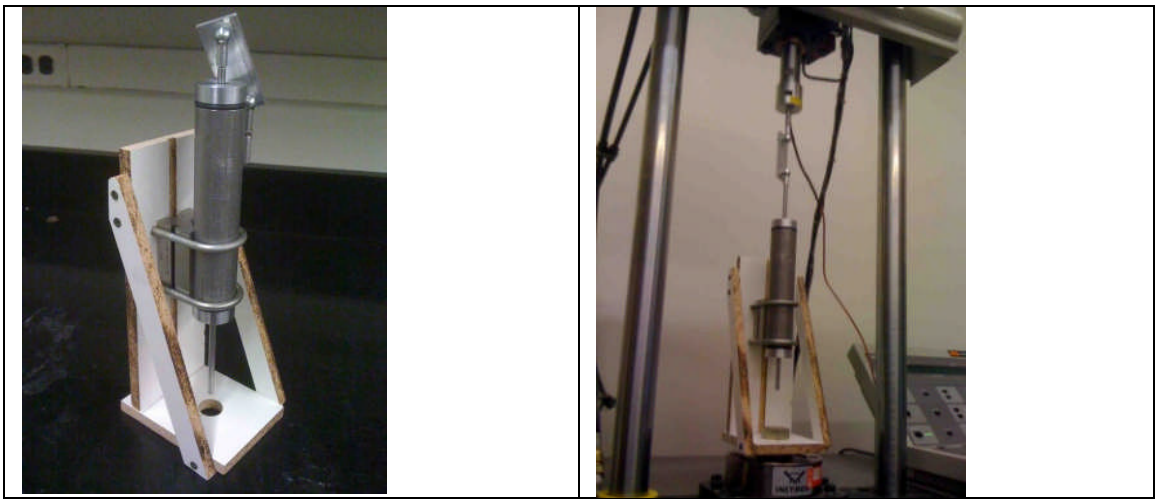

Figure 13: The damper in the Instron testing machine – direct attachment

Figure 14: The damper in the Instron machine: Lever attachment arrangement

Typical force – velocity results obtained with the levered attachment are shown in Figure 15. As the figure shows, the simple mathematical model captures the overall behavior regarding order of magnitude and shape of curve, but the experimental results show significant drift with time as oscillation cycles are repeated. This seems to be due to a steady drift in acceleration measurements, which upon integration to obtain velocity lead to steadily shifting the velocity-time curve with time.

Work is currently underway to stiffen the lever system used to attach the damper to the Instron machine, test in a machine that would allow direct attachment and larger stroke, and improvement of the design of the piston head. CFD modeling of the damper will, hopefully, lead to better insight. With the damper characteristics fully validated and with a mathematical model of the damper that will capture its behavior accurately, tests of the tail/rudder system with the damper and without hinge stiffness will be carried out.

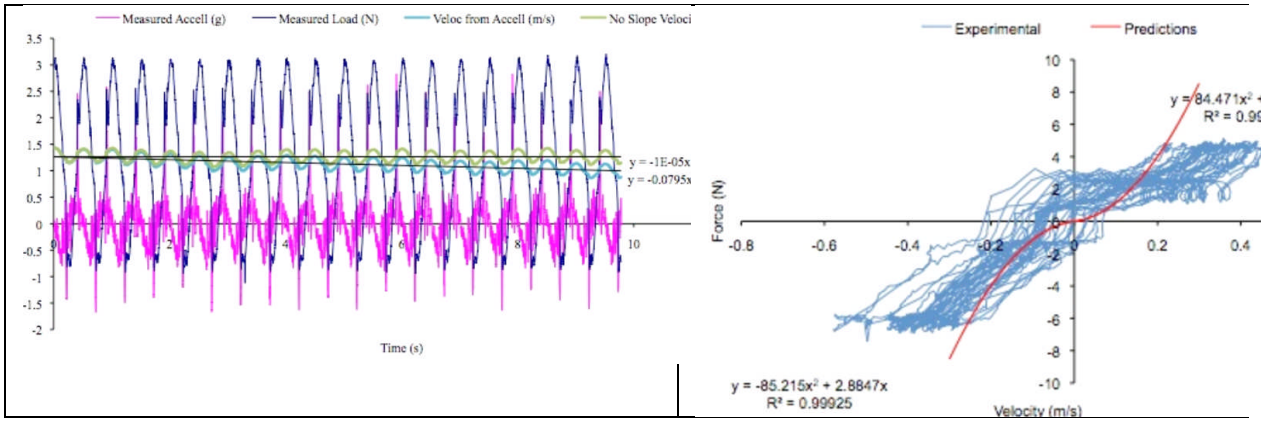

Figure 15: Measured force and acceleration and resultant force vs velocity curves for the damper (2 Hz, amplitude 26.311 mm)

References

1. Demasi, L., and Livne, E., "Dynamic Aeroelasticity of Structurally Nonlinear Configurations Using Linear Modally Reduced Aerodynamic Generalized Forces", AIAA Journal, 2009, Vol. 47, No.1, pp. 70-90.
2. Styuart, A., Mor, M., Livne, E., and Lin, K., "Risk Assessment of Aeroelastic Failure Phenomena in Damage Tolerant Composite Structures", submitted for publication, AIAA Journal.
3. Demasi, L., and Livne, E., "Aeroelastic Coupling of Geometrically Nonlinear Structures and Linear Unsteady Aerodynamics: Two Formulations", Journal of Fluids and Structures, Vol. 25, Issue 5, July 2009, Pages 918-935.
4. Demasi, L., and Livne, E., "Static Aeroelasticity of Joined Wing Configurations", AIAA Paper 2006-1639, 47th AIAA / ASME / ASCE / AHS / ASC Structures, Structural Dynamics, and Materials Conference, Newport, RI, May 2006.
5. Demasi, L., and Livne, E., "Performance of Order Reduction Techniques in the Case of Structurally Nonlinear Joined-Wing Configurations", AIAA Paper 2007-2052, 48th AIAA / ASME / ASCE / AHS / ASC Structures, Structural Dynamics, and Materials Conference, Honolulu, Hawaii, Apr. 23-26, 2007
6. Styuart, A., Mor, M., Livne, E., and Lin, K., "Risk Assessment of Aeroelastic Failure Phenomena in Damage Tolerant Composite Structures", AIAA Paper 2007-1981, 48th AIAA / ASME / ASCE / AHS / ASC Structures,

Structural Dynamics, and Materials Conference, Honolulu, Hawaii, Apr. 23-26, 2007

7. Demasi, L., and Livne, E., “Dynamic Aeroelasticity of Structurally Nonlinear Joined Wing Configurations Using Linear Modally Reduced Aerodynamic Generalized Forces”, AIAA Paper 2007-2105, 48th AIAA / ASME / ASCE / AHS / ASC Structures, Structural Dynamics, and Materials Conference, Honolulu, Hawaii, Apr. 23-26, 2007
8. Demasi, L., and Livne, E., “Dynamic Aeroelasticity Coupling Full Order Geometrically Nonlinear Structures and Full Order Linear Unsteady Aerodynamics - The Joined Wing Case”, AIAA-2008-1818, 49th AIAA / ASME / ASCE / AHS / ASC Structures, Structural Dynamics, and Materials Conference, Schaumburg, IL, Apr. 7-10, 2008
9. Demasi, L., and Livne, E., “Aeroelastic Coupling of Geometrically Nonlinear Structures and Linear Unsteady Aerodynamics: Two Formulations”, AIAA-2008-1758, 49th AIAA / ASME / ASCE / AHS / ASC Structures, Structural Dynamics, and Materials Conference, Schaumburg, IL, Apr. 7-10, 2008
10. Styuart, A., Demasi, L., Livne, E., and Lin, K., “Probabilistic Modeling of Aeroelastic Life Cycle for Risk Evaluation of Composite Structures”, AIAA-2008-2300, 49th AIAA / ASME / ASCE / AHS / ASC Structures, Structural Dynamics, and Materials Conference, Schaumburg, IL, Apr. 7-10, 2008
11. Styuart, A.V., Lin, K.Y., and Livne, E., “Probabilistic Modeling of Structural / Aeroelastic Life Cycle for Reliability Evaluation of Damage Tolerant Composite Structures”, ICAS 2008-7.1.1, 26th Congress of the International Council of the Aeronautical Sciences,14-19 September 2008, Anchorage, Alaska.
12. Paltera, F., Tuttle, M., and Livne, E., "Flutter Response To Damage Of Composite Aircraft Control Surfaces", 2009-407 session 069 SEM Annual Conference & Exposition on Experimental and Applied Mechanics, Albuquerque, New Mexico USA, June 1 - 4, 2009.
13. Tang, D., Dowell, E.H., and Virgin, L.N., " Limit cycle oscillations of an airfoil with a control surface". Journal of Fluids and Structures, 12:839–858, 1998.
14. Vipperman, J.S., R. L. Clark, R.L., Conner, M., and Dowell, E.H., "Experimental active control of a typical section using a trailing-edge flap", Journal Of Aircraft, 1998, vol. 35 no. 2, pp. 224 -- 229 .
15. Kholodar, D.B., and Dowell, E.H., "Behavior of Airfoil with Control Surface Freeplay for Nonzero Angles of Attack", AIAA Journal, 1999, vol.37 no.5, pp. 651-653.
16. Clark, R.L., Dowell, E.H., and Frampton, K.D., "Control of a three-degree-of-freedom airfoil with limit-cycle behavior", Journal Of Aircraft, 2000, vol. 37 no. 3, pp. 533 -- 536 .
17. Tang, D., Kholodar, D., and Dowell, E.H., "Nonlinear Response of Airfoil Section with Control Surface Freeplay to Gust Loads", AIAA Journal, 2000, vol.38 no.9, pp. 1543-1557.
18. Dowell, D., and Tang, D., "Nonlinear Aeroelasticity and Unsteady Aerodynamics", AIAA Journal, 2002, vol.40 no.9, pp. 1697-1707.
19. Dowell, E.H., Edwards, J., and Strganac, T., "Nonlinear Aeroelasticity", Journal of Aircraft, 2003, vol.40 no.5, pp. 857-874.
20. Liu, L., and Dowell, E.H., "Harmonic Balance Approach for an Airfoil with a Freeplay Control Surface", AIAA Journal, 2005, vol.43 no.4, pp. 802-815.
21. Gordon, J.T., Meyer, E.E., and Minogue, R.L., ".Nonlinear stability analysis of control surface flutter with free-play effects", Journal of Aircraft, 45(6):1904–1916, November–December 2008.
22. Gordon, J., "Nonlinear damping effects on control surface flutter of a typical section airfoil", International Forum on Aeroelasticity and Structural Dynamics, Seattle, WA, June 2009, Paper IFASD-2009-056.